Knight Shifts and Band Structure in the Lead-Salt Semiconductors*

STEPHEN D. SENTURIA, ARTHUR C. SMITH, AND C. ROBERT HEWES
Center for Materials Science and Engineering, and Department of Electrical Engineering, Massachusetts Institute of Technology, Cambridge, Massachusetts 02139

AND

J. ANTON HOFMANN AND PAUL L. SAGALYN
Materials Science Division, Army Materials and Mechanics Research Center, Watertown, Massachusetts 02172

(Received 19 December 1969)

The temperature and carrier-concentration dependences of the Pb^{207} and Te^{125} Knight shifts have been measured in both n- and p-type PbTe. Qualitatively similar data have been reported by others for Pb^{207} in PbSe. The very large shifts of Pb^{207} in p-type material and the relatively small shifts of Te^{125} in n-type material are attributed to an s-character contact interaction with the carriers of the valence and conduction bands, respectively. The sign of the isotropic g factor g_{eff} is negative in the L-point valence band and positive in the L-point conduction band, in agreement with the results of $\mathbf{k}\cdot\mathbf{p}$ perturbation theory. The temperature dependence of the Knight shift is ascribed to the motion of the Fermi level, the temperature dependence of the energy gap and related band parameters, and to the shift in carriers from the L-point valence band to a second valence band at temperatures above about 200°K. The localized orbital hyperfine interaction is suggested as the source of the Knight shifts of Pb^{207} in n-type material and Te^{125} in p-type material.

I. INTRODUCTION

THE lead-salt semiconductors, PbS, PbSe, and PbTe, comprise an interesting class of materials for a NMR study because of the relatively large Knight shifts observed in these materials and because of the wealth of experimental and theoretical information available on the energy-band structures. Our goal in this study is to relate the temperature and carrier-concentration dependences of the various Knight shifts to the characteristics of the lead-salt energy bands.

A number of workers have reported experimental data on Pb^{207} nuclear resonances in various lead-salt samples. Weinberg's initial observation[1] of the Pb^{207} resonance in PbS, PbSe, and PbTe at room temperature was followed by Weinberg and Callaway's temperature-dependent study[2,3] of the Pb^{207} resonance in one p-type sample of PbTe. Bailey[4] has attempted to relate their results to the relativistic augmented-plane-wave (APW) energy-band calculations for PbTe. Sapoval,[5,6] using helicon wave propagation in bulk samples at 1.2°K, and the present group,[7–9] using standard NMR absorption in powdered samples at temperatures in the range 55–525°K, have extended the study of Pb^{207} in PbTe to a range of carrier concentrations. In PbSe, Pifer's inconclusive study[10] was followed by Lee, Liesegang, and Phipps's study[11] of Pb^{207} in several PbSe powders. Measurements of the Te^{125} resonance in PbTe have been made both by Sapoval[5,6] and by the present group.

The picture that emerges from these various studies is only partially clear. Sample preparation and characterization has been and continues to be a serious and difficult problem. Furthermore, various errors in previous theoretical discussions have led to widely varying interpretations of the large Pb^{207} Knight shift encountered in p-type material. While the origin of this shift has been consistently ascribed to the contact interaction between the lead nuclear moment and the valence-band holes, the theory of the temperature and carrier-concentration dependence of the contact interaction Knight shift has not been correctly applied to the data. In this paper, we present a detailed derivation of the contact interaction Knight shift in the lead salts, including the use of valence- and conduction-band states which have been split and mixed by the spin-orbit interaction. Particular attention is paid to the sign of the g factor and how it appears in the final result.

Before proceeding to the detailed theory, it should be noted that for the currently assumed lead-salt band structure, the contact interaction is expected to shift the Pb^{207} resonance in p-type material, and to a lesser extent, the Te^{125} resonance in n-type material. The situations for Pb^{207} in n-type material and Te^{125} in p-type material are unclear; in these latter cases, we shall comment briefly on the Knight shifts which might arise from the localized orbital hyperfine interaction.

II. THEORY

A. Terminology

In the derivation which follows, the nuclear magnetic moment is represented by $\boldsymbol{\mu}_N=\gamma\hbar\mathbf{I}$, where γ is the

* Work supported by the Office of Naval Research and by the Army Materials and Mechanics Research Center.

[1] I. Weinberg, J. Chem. Phys. **36**, 1112 (1962).
[2] I. Weinberg and J. Callaway, Nuovo Cimento **24**, 190 (1962).
[3] I. Weinberg, J. Chem. Phys. **39**, 492 (1963).
[4] P. T. Bailey, Phys. Rev. **170**, 723 (1968).
[5] B. Sapoval, Phys. Rev. Letters **17**, 241 (1966).
[6] B. Sapoval, thesis, Ecole Polytechnique, 1968 (unpublished); J. Phys. (Paris) Suppl. **29**, C4 (1968).
[7] S. D. Senturia, A. C. Smith, and P. L. Sagalyn, Bull. Am. Phys. Soc. **12**, 574 (1967).
[8] A. C. Smith, S. D. Senturia, and C. R. Hewes, Bull. Am. Phys. Soc. **14**, 329 (1969).
[9] S. D. Senturia, A. C. Smith, C. R. Hewes, J. A. Hofmann, and P. L. Sagalyn, Bull. Am. Phys. Soc. **14**, 329 (1969).
[10] J. H. Pifer, Phys. Rev. **157**, 272 (1967).
[11] K. Lee, J. Liesegang, and P. B. P. Phipps, Phys. Rev. **161**, 322 (1967).

gyromagnetic ratio and $\mathbf{I}$ is the nuclear spin. The free-electron magnetic moment is represented by $\boldsymbol{\mu}_e = -g_0\beta_0\mathbf{S}$, where g_0 is the free-electron g value $(+2)$, β_0 is the Bohr magneton, and $\mathbf{S}$ is the electron spin. In calculating shifts of resonance lines, we refer to experiments done at some constant frequency ν_0. We define the reference field to be the external magnetic field which must be applied to a carrier-free sample in order to resonate the nucleus of interest at the frequency ν_0. Thus, the reference field, denoted by H_r, which can be temperature dependent, includes all the normal contributions to the "chemical shift," but does not include any shift produced by the carriers. If we call H_s the external field which must be applied to a real sample in order to resonate the nuclei at the constant frequency ν_0, then the quantity $H_r - H_s$ represents the additional effect of the carriers on the location of the nuclear resonance. This field shift, called the Knight shift K, is usually proportional to H_s, and is therefore usually expressed in dimensionless form

$$K = (H_r - H_s)/H_s. \tag{1}$$

For convenience in comparing theory and experiment, we shall calculate directly the field shift corresponding to $H_r - H_s$. The sign in Eq. (1) is chosen in accordance with the usual convention, in that a positive Knight shift corresponds to $H_s < H_r$. In semiconductors, where one can vary the carrier concentration, one can measure the H_r by extrapolating the carrier-concentration dependence of H_s to zero carriers. Where such an extrapolation is possible, it is not necessary to rely either on diamagnetic standards or on calculated corrections in order to determine unambiguously both the sign and the magnitude of the Knight shift.

B. Contact Interaction

The Hamiltonian representing the contact interaction coupling between a nucleus and an electron is written as

$$\mathcal{H}_c = \frac{8}{3}\pi g_0\beta_0\gamma\hbar\mathbf{I}\cdot\mathbf{S}\delta(\mathbf{r}), \tag{2}$$

where $\delta(\mathbf{r})$ is a δ function at the nuclear position $(\mathbf{r}=0)$. In the presence of an external magnetic field $\mathbf{H}_s$, the contact interaction represents a weak perturbation of the nuclear Zeeman energies. Since the nuclear spin $\mathbf{I}$ remains quantized along $\mathbf{H}_s$, $\langle I_x\rangle = \langle I_y\rangle = 0$, and only the term proportional to S_z (the z axis is taken along $\mathbf{H}_s$) contributes to a shift of the nuclear Zeeman energies. When the contributions from all occupied electron states are summed, the contact interaction can be represented as an additional effective field H_c, which is in the direction of $\mathbf{H}_s$, and is given by

$$H_c = -\frac{8}{3}\pi g_0\beta_0 \sum_{\mathbf{k},\sigma} \langle\psi_{\mathbf{k},\sigma}|S_z\delta(\mathbf{r})|\psi_{\mathbf{k},\sigma}\rangle f(\mathbf{k},\sigma,\mathbf{H}_s), \tag{3}$$

where $|\psi_{\mathbf{k},\sigma}\rangle$ is a single-particle valence- or conduction-band state with wave vector $\mathbf{k}$ and Kramers-doublet spin index $\sigma(=\pm 1)$, and where $f(\mathbf{k},\sigma,\mathbf{H}_s)$ is the Fermi function probability that $|\psi_{\mathbf{k},\sigma}\rangle$ is occupied when the sample is placed in an external field $\mathbf{H}_s$. In simplest terms, H_c becomes nonzero when $f(\mathbf{k}, +1, \mathbf{H}_s) \neq f(\mathbf{k}, -1, \mathbf{H}_s)$; that is, when the carriers are polarized by the external field. And it is the quantity H_c which is to be compared with the experimentally determined quantity $H_r - H_s$.

Several features of the lead-salt energy bands require us to use great care in evaluating the matrix elements of $S_z\delta(\mathbf{r})$ and the sum over states of Eq. (3). We shall illustrate these features with specific reference to the L-point band-edge states as summarized by Rabii[12] and by Mitchell and Wallis.[13]

First, the valence- and conduction-band states are mixed by spin-orbit coupling so that $|\psi_{\mathbf{k},\sigma}\rangle$ cannot be represented by a simple Bloch function times a spin function. Instead, $|\psi_{\mathbf{k},\sigma}\rangle$ is a linear combination of Bloch-state–spin-state products containing both "up-spin" and "down-spin" parts, either of which might contribute to the matrix element of $S_z\delta(\mathbf{r})$. Mitchell and Wallis[13] have shown that for the states which contribute to the valence- and conduction-band edges at the L point, it is possible to make an unambiguous identification of the $\sigma = +1$ and the $\sigma = -1$ partners of the Kramers doublets using a convention based on the sense of circular polarization of the radiation absorbed in a spin-resonance experiment.

Second, there are four valleys at the $\langle 111\rangle$ zone edges. In the absence of a magnetic field, the sum over $\mathbf{k}$ could be split up first into a sum over four equivalent $\mathbf{k}$ vectors, one in each of the four valleys, and then a sum over all the $\mathbf{k}$ vectors within a single valley. But when the sample is placed in an arbitrarily oriented external magnetic field $\mathbf{H}_s$, the four valleys are not, in general, equivalent. Neither the matrix elements of $S_z\delta(\mathbf{r})$ nor the Fermi population factors will be identical in all four valleys, so the sum over valleys must be carried out, valley by valley, for the assumed direction of $\mathbf{H}_s$. Since the cubic symmetry of the lead salts requires that the final result for H_c be independent of the orientation of $\mathbf{H}_s$, one may choose $\mathbf{H}_s$ in any direction. Therefore, we may simplify the problem by taking $\mathbf{H}_s$ along [001], in which case the four valleys are fully equivalent.

We now proceed to evaluate H_c. It is convenient to treat the problem of the four valleys by evaluating the vector operator $\mathbf{S}_n\delta(\mathbf{r})$ in each of four symmetrically equivalent coordinate systems $(x_n, y_n, z_n; n = 1, 2, 3, 4)$ with each z_n axis along the principal axis of one of the four valleys. Following Mitchell and Wallis,[13] we take the x_1, y_1, z_1 axes along the $[\bar{1}\bar{1}2]$, $[1\bar{1}0]$, and $[111]$ crystallographic directions, respectively. The remaining three coordinate systems are generated by fourfold rotations about the z axis [001]. The expectation value

[12] Sohrab Rabii, Phys. Rev. **167**, 801 (1968).
[13] D. L. Mitchell and R. F. Wallis, Phys. Rev. **151**, 581 (1966).

of $\mathbf{S}_n\delta(\mathbf{r})$, weighted by the correct Fermi population factor, will then be projected along the direction of the external magnetic field to obtain the contribution of the nth valley to the summand in Eq. (3).

In each valley, we define the spin functions

$$(\uparrow)=\begin{pmatrix}1\\0\end{pmatrix} \quad \text{and} \quad (\downarrow)=\begin{pmatrix}0\\1\end{pmatrix}$$

for S_{z_n} along the appropriate z_n axis. (The eigenvalues of S_{z_n} are $\pm\frac{1}{2}$ in this basis.) In each valley, one of the spin-orbit mixed states of the Kramers doublet can then be written in terms of two functions $u_{\mathbf{k}}(\mathbf{r})$ and $\bar{u}_{\mathbf{k}}(\mathbf{r})$:

$$|\Psi_{\mathbf{k},\alpha}\rangle=\Phi_{\mathbf{k}}(a_{\mathbf{k}}u_{\mathbf{k}}\uparrow+\bar{a}_{\mathbf{k}}\bar{u}_{\mathbf{k}}\downarrow), \tag{4}$$

where $u_{\mathbf{k}}(\mathbf{r})$ and $\bar{u}_{\mathbf{k}}(\mathbf{r})$ are normalized in a volume Ω, and transform according to different irreducible representations of the single group; the coefficients $a_{\mathbf{k}}$ and $\bar{a}_{\mathbf{k}}$ satisfy $|a_{\mathbf{k}}|^2+|\bar{a}_{\mathbf{k}}|^2=1$, and $\Phi_{\mathbf{k}}$ is a phase factor which cancels out of all matrix elements. The other spin state at the same $\mathbf{k}$ vector is obtained by applying time reversal and inversion to Eq. (4).[13] Note that it is not possible for both $u_{\mathbf{k}}(0)$ and $\bar{u}_{\mathbf{k}}(0)$ to be nonzero. [Since $u_{\mathbf{k}}(\mathbf{r})$ and $\bar{u}_{\mathbf{k}}(\mathbf{r})$ transform according to different irreducible representations of the single-group states before spin-orbit coupling is considered, both components cannot have s-state symmetry.] Using the Kramers states just defined, we can evaluate the magnetic part of the effective-mass Hamiltonian.[14] The eigenvalues of this 2×2 matrix are given by

$$\Delta E_{\mathbf{k},\sigma}=\tfrac{1}{2}\sigma\beta_0(\lambda_{x_n}{}^2g_\perp{}^2+\lambda_{y_n}{}^2g_\perp{}^2+\lambda_{z_n}{}^2g_{\parallel}{}^2)^{1/2}H_s, \tag{5}$$

where the spin index $\sigma=\pm1$; the direction cosines $\lambda_{\gamma_n}(\gamma=x,\,y,\,z)$ are the cosines between the applied field direction and the principal axes of the valley ($\mathbf{i}_{\gamma_n}$).

The $\mathbf{g}$ tensor is defined in the valley coordinate system:

$$\mathbf{g}(\mathbf{k})=\begin{bmatrix}g_\perp(\mathbf{k}) & 0 & 0\\ 0 & g_\perp(\mathbf{k}) & 0\\ 0 & 0 & g_{\parallel}(\mathbf{k})\end{bmatrix}. \tag{6}$$

The expectation values of $\mathbf{S}_n\delta(\mathbf{r})$ for the eigenfunctions corresponding to the eigenvalues of Eq. (5) are given by

$$\langle\Psi_{\mathbf{k},\sigma}|\,\mathbf{S}_n\delta(\mathbf{r})\,|\Psi_{\mathbf{k},\sigma}\rangle = \frac{\sigma A(\mathbf{k})}{2}\frac{(\lambda_{x_n}g_\perp\mathbf{i}_{x_n}+\lambda_{y_n}g_\perp\mathbf{i}_{y_n}+\lambda_{z_n}g_{\parallel}\mathbf{i}_{z_n})}{(\lambda_{x_n}{}^2g_\perp{}^2+\lambda_{y_n}{}^2g_\perp{}^2+\lambda_{z_n}{}^2g_{\parallel}{}^2)^{1/2}}, \tag{7}$$

where

$$A(\mathbf{k})=|a_{\mathbf{k}}u_{\mathbf{k}}(0)|^2-|\bar{a}_{\mathbf{k}}\bar{u}_{\mathbf{k}}(0)|^2. \tag{8}$$

Since the $\mathbf{g}$ tensor for each valley is nonisotropic, it is seen that the direction of quantization of spin for each valley will not, in general, be parallel to the applied field. Note that $A(\mathbf{k})$, which corresponds to the "square of the wave function at the origin" in the usual contact interaction derivation, might be either positive or negative, depending on whether $u_{\mathbf{k}}$ or $\bar{u}_{\mathbf{k}}$ is the wave-function component transforming like an s state about the nucleus of interest. It will turn out that for both the valence band about lead and for the conduction band about the chalcogenide, it is the $u_{\mathbf{k}}$ component which possesses s character. At this point in the discussion, however, we shall carry both components of $A(\mathbf{k})$.

Having evaluated the matrix elements of $\mathbf{S}_n\delta(\mathbf{r})$ in each valley, we proceed to the population factors $f(\mathbf{k},\sigma,\mathbf{H}_s)$. Assuming that $\Delta E_{\mathbf{k},\sigma}$, the shift in energy of the state $|\Psi_{\mathbf{k},\sigma}\rangle$ in the magnetic field $\mathbf{H}_s$, is small compared to kT (or in the case of degenerate carrier statistics at low temperature, small compared to the Fermi energy), we can expand the Fermi function

$$f(\mathbf{k},\sigma,\mathbf{H}_s)=f(E(\mathbf{k}))+\left(\frac{df}{dE}\bigg|_{H_s=0}\right)\Delta E_{\mathbf{k},\sigma}, \tag{9}$$

where $f(E(\mathbf{k}))$ is the Fermi function in the absence of the magnetic field and $E(\mathbf{k})$ is the band energy measured from the band edge into the band. Using Eqs. (5), (7), and (9), and performing the sum over the spin index $\sigma=\pm1$, we find

$$\sum_\sigma\langle\Psi_{k,\sigma}|\,\mathbf{S}_n\delta(\mathbf{r})\,|\Psi_{k,\sigma}\rangle f(\mathbf{k},\sigma,\mathbf{H}_s)=\tfrac{1}{2}\beta_0H_sA(\mathbf{k})(\lambda_{x_n}g_\perp\mathbf{i}_{x_n} +\lambda_{y_n}g_\perp\mathbf{i}_{y_n}+\lambda_{z_n}g_{\parallel}\mathbf{i}_{z_n})\left(\frac{df}{dE}\bigg|_{H_s=0}\right). \tag{10}$$

Taking the scalar product of both sides of Eq. (10) with $\mathbf{i}_z$, a unit vector along the direction of the applied field, then gives for the nth valley

$$\sum_\sigma\langle\Psi_{\mathbf{k},\sigma}|\,S_z\delta(\mathbf{r})\,|\Psi_{\mathbf{k},\sigma}\rangle f(\mathbf{k},\sigma,\mathbf{H}_s)=\tfrac{1}{2}\beta_0H_sA(\mathbf{k})(\lambda_{x_n}{}^2g_\perp +\lambda_{y_n}{}^2g_\perp+\lambda_{z_n}{}^2g_{\parallel})\left(\frac{df}{dE}\bigg|_{H_s=0}\right). \tag{11}$$

For our choice of applied field along [001], $\lambda_{x_n}=\sqrt{2}/\sqrt{3}$, $\lambda_{y_n}=0$, $\lambda_{z_n}=1/\sqrt{3}$, independent of n. We see from Eq. (11), therefore, that the contribution from each valley to the sum over $\mathbf{k}$ of Eq. (3) is identical, as expected, and Eq. (3) can now be written

$$H_c=-\frac{16\pi g_0\beta_0{}^2H_s}{3}\times\sum_{\mathbf{k}}A(\mathbf{k})\tfrac{1}{3}[2g_\perp(\mathbf{k})+g_{\parallel}(\mathbf{k})]\left(\frac{df}{dE}\bigg|_{H_s=0}\right), \tag{12}$$

where the sum over $\mathbf{k}$ now runs over one valley. If one then makes the very reasonable assumption that the $\mathbf{k}$ dependence of $A(\mathbf{k})$, $g_\perp(\mathbf{k})$, and $g_{\parallel}(\mathbf{k})$ are contained in the energy $E(\mathbf{k})$, we can convert the sum to an integral over the density of states and integrate by

[14] Y. Yafet, in *Solid State Physics*, edited by F. Seitz and D. Turnbull (Academic Press Inc., New York, 1963), Vol. 14, pp. 1–98.

parts to obtain

$$H_c = \frac{16\pi g_0 \beta_0^2 H_s \Omega}{3} \int_0^\infty f(E,E_F) \frac{d}{dE} \times [A(E) g_{\text{eff}}(E) \rho(E)]\, dE, \quad (13)$$

where E is the energy measured from the band edge into the band,

$$A(E) = |a_E u_E(0)|^2 - |\bar{a}_E \bar{u}_E(0)|^2,$$
$$g_{\text{eff}}(E) = \tfrac{1}{3}[2g_\perp(E) + g_\parallel(E)],$$

where $\rho(E)$ is the density of states per unit volume for a single valley and a single spin, E_F is the Fermi energy, and Ω is the normalization volume for $u_E(\mathbf{r})$ and $\bar{u}_E(\mathbf{r})$.

C. Theoretical Estimates of H_c

The quantity H_c, which is to be compared to the experimentally determined quantity $H_r - H_s$, defined earlier, depends on the specific energy-band model through the quantities $g_{\text{eff}}(E)$, $A(E)$, and $\rho(E)$. It is now appropriate, therefore, to introduce specific features of various band models, and then to compare the theoretical estimates of H_c with experiment.

1. Sign of Knight Shift

The sign of H_c is most easily discussed in the context of a very simple case: degenerate material at low temperature, a case which arises in the lead salts because of the absence of carrier freeze-out.[15] In this case, one obtains

$$H_c = (16\pi g_0 \beta_0^2 H_s \Omega/3) A(E_F) g_{\text{eff}}(E_F) \rho(E_F), \quad (14)$$

where $\rho(E_F)$ is the density of states at the Fermi energy. This formula differs from the formula used by Sapoval[6] in the inclusion of the spin-orbit mixed wave functions through the quantity A.

The contact-interaction Knight shift is seen to depend on the *product* of A and g_{eff}. We recall that the sign of A depends on which component of the Kramers-doublet wave function has s character. The lead-salt valence-band states at the L point have L_6^+ symmetry and arise from the spin-orbit mixing of several $L_6^+(L_1^+)$ states and one $L_6^+(L_3^+)$ state.[12,13] Mitchell and Wallis[13] have shown that in order for the $\sigma = \pm 1$ Kramers-doublet partners to transform like "spin-up" and "spin-down" states, respectively, in the sense that the $\sigma = -1$ state is coupled to the $\sigma = +1$ state by the raising operator $\sigma_+ = \frac{1}{2}(\sigma_x + i\sigma_y)$, then the $L_6^+(L_1^+)$ component of the valence-band state must be associated with u_k and the $L_6^+(L_3^+)$ component with $\bar{u}_k$. Since it is the $L_6^+(L_1^+)$ component, hence the u_k component, which has s character about the lead nucleus,[16] A is positive for the contact-interaction Knight shift of the lead resonance in p-type material.

Similarly, Mitchell and Wallis[13] have shown that for the conduction band the $L_6^-(L_2^-)$ component must be associated with u_k and the $L_6^-(L_3^-)$ component with $\bar{u}_k$. Since the $L_6^-(L_2^-)$ states have s character about the chalcogenide site, A is also positive for the contact-interaction shift of the chalcogenide resonance in n-type samples.

In summary, the signs of the Knight shifts of Pb^{207} in p-type material and of S^{33}, Se^{77}, or Te^{125} in n-type material are the same as the signs of g_{eff} for the valence band and conduction bands, respectively. It will be seen below that the Pb^{207} Knight-shift data clearly show $g_{\text{eff}} < 0$ in the valence band; based on our more limited Te^{125} data, we conclude $g_{\text{eff}} > 0$ in the conduction band.

2. Temperature and Carrier-Concentration Dependence of Knight Shift

At sufficiently low temperatures, the carrier-concentration dependence of H_c is contained entirely in the Fermi level through the factor $[A(E_F) g_{\text{eff}}(E_F) \rho(E_F)]$ of Eq. (14). Sapoval,[6] using his measurements of H_c versus carrier concentration for Pb^{207} in p-type PbTe at 1.2°K, has explicitly demonstrated the nonparabolicity of the L-point valence band, and has attempted to relate the observed Knight shift to the various parameters in the nonellipsoidal, nonparabolic band model of Cohen[17] as applied to PbTe by Cuff, Ellett, and Kuglin.[18] Our calculation of the Knight shift at higher temperatures[8,9] employed a similar band model (see below).

For investigations at other than very low temperatures, one must take account of the fact that as the temperature of a sample is increased from the degenerate case near $T = 0$, the Fermi level must move out of the band. This motion of the Fermi level is a major mechanism producing the temperature dependence of the contact-interaction Knight shift.[8] Other important features are the strongly temperature-dependent lead-salt energy gaps, which modify the nonparabolic energy bands as functions of temperature, and the importance of a second valence band, at least in lead telluride, at temperatures above about 200°K. We shall take up these issues in sequence.

3. Motion of Fermi Level

If the total carrier concentration in the sample is n, the carrier concentration corresponding to a single valley and a single spin state is $\frac{1}{8}n$, and this is related to the density of states per unit volume for a single valley and single spin state, $\rho(E)$, by

$$\frac{n}{8} = \int_0^\infty f(E,E_F) \rho(E)\, dE. \quad (15)$$

[15] R. S. Allgaier and W. W. Scanlon, Phys. Rev. **111**, 1029 (1958); N. J. Parada and G. W. Pratt, Jr., Phys. Rev. Letters **22**, 180 (1969).

[16] J. O. Dimmock and G. B. Wright, Phys. Rev. **135**, A821 (1964).

[17] Morrel H. Cohen, Phys. Rev. **121**, 387 (1961).

[18] K. F. Cuff, M. R. Ellett, and C. D. Kuglin, in *Proceedings of the International Conference on the Physics of Semiconductors, Exeter, 1962* (The Institute of Physics and the Physical Society, London, 1962), p. 316.

Since n is fixed and $f(E,E_F)$ is an explicit function of temperature, this relation determines the motion of the Fermi level implicitly as a function of temperature. Once $E_F(T)$ is determined, it can then be inserted into the integral in Eq. (13).

The quantitative effect of the motion of the Fermi level on H_c is most easily demonstrated by momentarily ignoring the other issues, such as the nonparabolic bands, the temperature-dependent energy gap, and the second valence band. Accordingly, we shall calculate the temperature and carrier-concentration dependence of H_c for a parabolic band presumed not to vary with temperature. We assume ellipsoidal constant-energy surfaces characterized by a transverse mass m_t and a longitudinal mass m_l. The parabolic density of states per unit volume for a single valley and single spin state, $\rho_p(E)$, is then

$$\rho_p(E)=\frac{1}{4\pi^2}\left(\frac{2m_l^{1/3}m_t^{2/3}}{\hbar^2}\right)^{3/2}E^{1/2}=CE^{1/2}\,, \qquad (16)$$

and Eq. (15), which determines $E_F(T)$, becomes

$$\tfrac{1}{8}n=C(kT)^{3/2}F_{1/2}(\eta)\,, \qquad (17)$$

where $\eta=E_F/kT$ and $F_{1/2}(\eta)$ is a tabulated Fermi integral.[19] Assuming for our simple parabolic model that A and $g_{\rm eff}$ are independent of E, Eq. (13) becomes

$$H_c=\frac{16\pi g_0\beta_0^2H_s\Omega A g_{\rm eff}C}{3}\int_0^\infty f(E,E_F)(\tfrac{1}{2}E^{-1/2})\,dE. \qquad (18)$$

The integral in Eq. (18) is simply $\frac{1}{2}(kT)^{1/2}F_{-1/2}(\eta)$. The quantity η is determined by Eq. (17).

We now apply Eq. (18) to the case of Pb^{207} in p-type PbTe. We take the valence-band masses to be $m_t=0.022m_0$ and $m_l=0.30m_0$.[18] In order to fix a scale for H_c which will later be easily related to our experimental data, we shall put $H_0=11\,220$ G (corresponding to our experiment). We take $|g_{\rm eff}|=25$, a reasonable value based on both experiment and theory,[12] and for A we shall estimate the value of $A(E)$ at the top of the valence band ($E=0$). We have seen above that for Pb in p-type PbTe, $\bar{u}_E(0)=0$; it follows that $A(0)=|a_0u_0(0)|^2$. With the usual definition of "s character," ξ, $|a_0u_0(0)|^2=\xi|\psi_A(0)|^2$, where $|\psi_A(0)|^2$ is the free-atom value. Bailey[4] has calculated ξ to be about 0.6 for the band-edge states of the PbTe valence band. In this calculation, Bailey used for $a_0u_0(\mathbf{r})$ the relativistically appropriate linear combination of Pb-sphere portions of PbTe APW wave functions, with these portions normalized in the APW Pb sphere[4,20] (the appropriate normalization volume in which to compare s character with the free-atom value).[21] This means, of course, that $u_0(\mathbf{r})$ is also normalized in this volume, so that for Ω in Eq. (18) we should use the Pb-sphere volume (radius $=3.1$ Bohr radii). Schawlow *et al.*[22] have determined the free-atom hyperfine interaction constant for Pb IV to be 2.60 cm^{-1}, from which $|\psi_A(0)|^2$ is approximately 6×10^{26} cm^{-3}. Bailey[4] has calculated that for the degree of ionization for Pb in PbTe, this number for $|\psi_A(0)|^2$ should be reduced by a factor of 0.46. We therefore estimate A to be

$$A=\xi(0.46)|\psi_A(0)|^2=1.7\times10^{26}\ \text{cm}^{-3}.$$

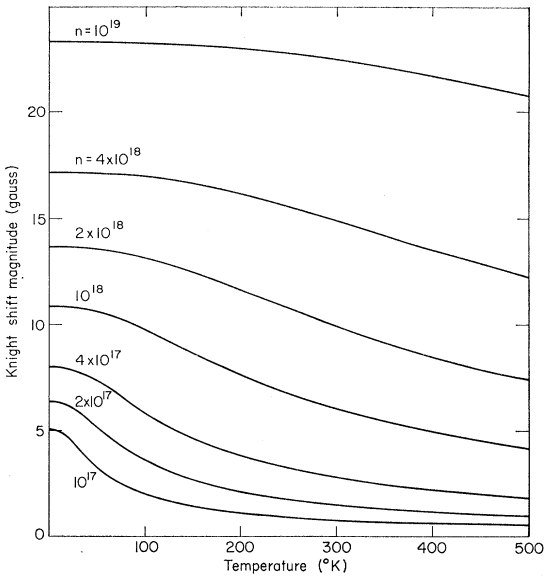

FIG. 1. Magnitude of the contact-interaction Knight shift as a function of temperature and carrier concentration as calculated for Pb^{207} in p-type PbTe. A parabolic-band approximation is used, along with numerical estimates of the band parameters appropriate to PbTe. The Knight shift in G corresponds to an experimental frequency of exactly 10 MHz.

Figure 1 shows the temperature and carrier-concentration dependence of the magnitude of the Knight shift $|H_c|$ for Pb^{207} in p-type PbTe obtained by using the above numerical values in Eqs. (16)–(18). The calculated $|H_c|$ at $T=0$ is seen to be about 23.2 G in a sample with 10^{19} carriers per cm^3. As temperature increases, the temperature dependence changes from the temperature-independent Knight-shift characteristic of degenerate systems to the $1/T$ dependence characteristic of nondegenerate semiconductors. H_c varies as $n^{1/3}$ for this parabolic model in the limit $T=0$, and varies as n in the high-temperature nondegenerate limit. It should be noted that the entire temperature dependence of H_c shown in Fig. 1 is due to the motion of the Fermi level with temperature.

[19] A. C. Beer, M. N. Chase, and P. F. Choquard, Helv. Phys. Acta **28**, 529 (1955).

[20] J. B. Conklin, Jr., L. E. Johnson, and G. W. Pratt, Jr., Phys. Rev. **137**, A1282 (1965).

[21] Sapoval (Ref. 6) used the entire PbTe unit cell for the normalization volume in which to compare s character with the Pb ion. Bailey (Ref. 4) discusses why a volume on the order of the APW Pb sphere is more appropriate.

[22] A. L. Schawlow, J. N. P. Hume, and M. F. Crawford, Phys. Rev. **76**, 1876 (1949).

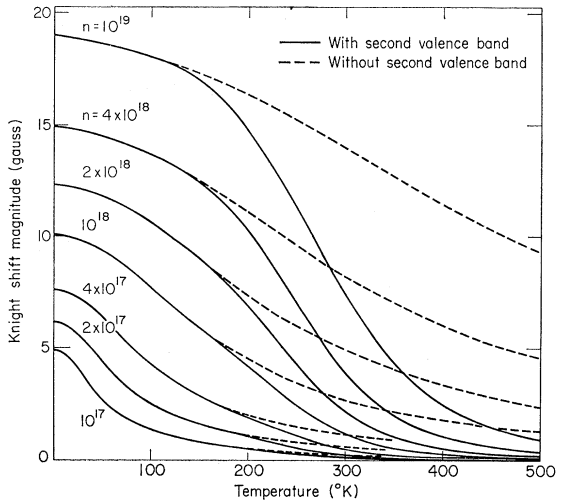

FIG. 2. Magnitude of the contact-interaction Knight shift as a function of temperature and carrier concentration as calculated for Pb^{207} in p-type PbTe. A nonparabolic-band model is used, both with and without the proposed valence band. The Knight shift in G corresponds to an experimental frequency of exactly 10 MHz.

4. *Nonparabolic Temperature-Dependent Bands*

Any realistic model for the lead salts must include at least nonparabolic energy bands and a temperature-dependent energy gap. One simple model with these features,[17,18] used by Sapoval for PbTe,[6] is not entirely adequate for a description of the bands because it explicitly neglects several interband couplings which are not negligible.[12] Nevertheless, in the spirit of Sapoval's analysis at 1.2°K, we shall calculate the temperature dependence of H_c for a model which differs only slightly from that used by Sapoval.

The nonparabolic models differ from the parabolic model in several ways. First, the density of states is given by

$$\rho(E)=\rho_p(E)[1+\tfrac{1}{3}(5+\mu)E/E_G], \qquad (19)$$

where μ is the ratio of the longitudinal band-edge masses in the valence and conduction bands and where E_G is the energy gap. Second, $g_\perp$ is assumed to be constant and small. Finally, $g_\parallel$ depends on energy as

$$g_\parallel(E)=g_\parallel(0)[1+\tfrac{1}{3}(5+\mu)E/E_G]^{-1}, \qquad (20)$$

where $g_\parallel(0)$ is the band-edge value of $g_\parallel$.

In our calculation, we have made E_G temperature dependent by using the "interaction gap"[16,23] value of 0.14 eV for E_G at $T=0$, and the linear temperature dependence 4×10^{-4} eV/°K as determined by Tauber *et al.*[24] Furthermore, we have assumed for simplicity that $g_{\rm eff}(E)$ has the energy dependence of $g_\parallel(E)$ in Eq. (20). Finally, we have taken[12] $|g_{\rm eff}(0)|=25$ and $\mu=1.6$ (Sapoval's use of $\mu=1$ affects the final result only slightly).

The temperature-dependent density of states of Eq. (19) is then used to locate the Fermi level as a function of temperature in Eq. (15). The resulting Fermi level is then used in Eq. (13) to calculate the magnitude of H_c. The results of this calculation are plotted as the dashed curves of Fig. 2. The primary effect of the nonparabolicity is to produce a deviation from the $n^{1/3}$ dependence at low temperature, an effect which has been well documented by Sapoval.[6] The temperature dependence is qualitatively similar to the parabolic band case.

5. *Second Valence Band*

On the basis of transport[25,26] and optical measurements[24] in PbTe, a second valence-band maximum has been postulated somewhere removed from the L point in the Brillouin zone. The APW band calculations indicate a secondary maximum on the Σ axis.[12] The energy gap between this secondary maximum and the conduction band is postulated to be independent of temperature, while the principal energy gap between the L-point valence band and the conduction band increases linearly with temperature. As a result, the secondary band, which is not occupied at $T=0$, becomes occupied as the temperature is increased. This secondary band is modeled as parabolic with a density-of-states effective mass equal to $1.2m_0$.[25] Because of this heavy mass, the g factors in this band are expected to be small. Since the Knight shift is proportional to the g factor, carriers in this band should not contribute significantly to the total Knight shift. We have assumed for simplicity that carriers in this second band produce *no* Knight shift. Using Tauber's measurement of the energy of this secondary band edge,[24] we can recompute the Fermi level at each temperature by invoking the constraint that the sum of the carriers in the L-point maximum and the secondary maximum must equal n. This Fermi level is then used to compute H_c as before. The results of this calculation are plotted as the solid curves of Fig. 2. Note that as the carriers shift out of the L-point maximum at temperatures above about 200°K, the Knight shift rapidly goes toward zero. We shall see below that this behavior is observed experimentally in p-type PbTe.

III. COMPARISON WITH EXPERIMENT

A. Pb^{207} NMR in PbTe

Except at liquid-helium temperatures, where Sapoval's method[5] of doing NMR with helicon waves in bulk samples can be used, it is necessary to perform

[23] K. F. Cuff, M. R. Ellett, C. D. Kuglin, and L. R. William, in *Proceedings of the International Conference on the Physics of Semiconductors* (Dunod Cie, Paris, 1964), p. 677.

[24] R. N. Tauber, A. A. Machonis, and I. B. Cadoff, J. Appl. Phys. **37**, 4855 (1966).

[25] R. S. Allgaier, J. Appl. Phys. **32**, 2185 (1961).

[26] R. S. Allgaier and B. B. Houston, Jr., J. Appl. Phys. **37**, 302 (1966).

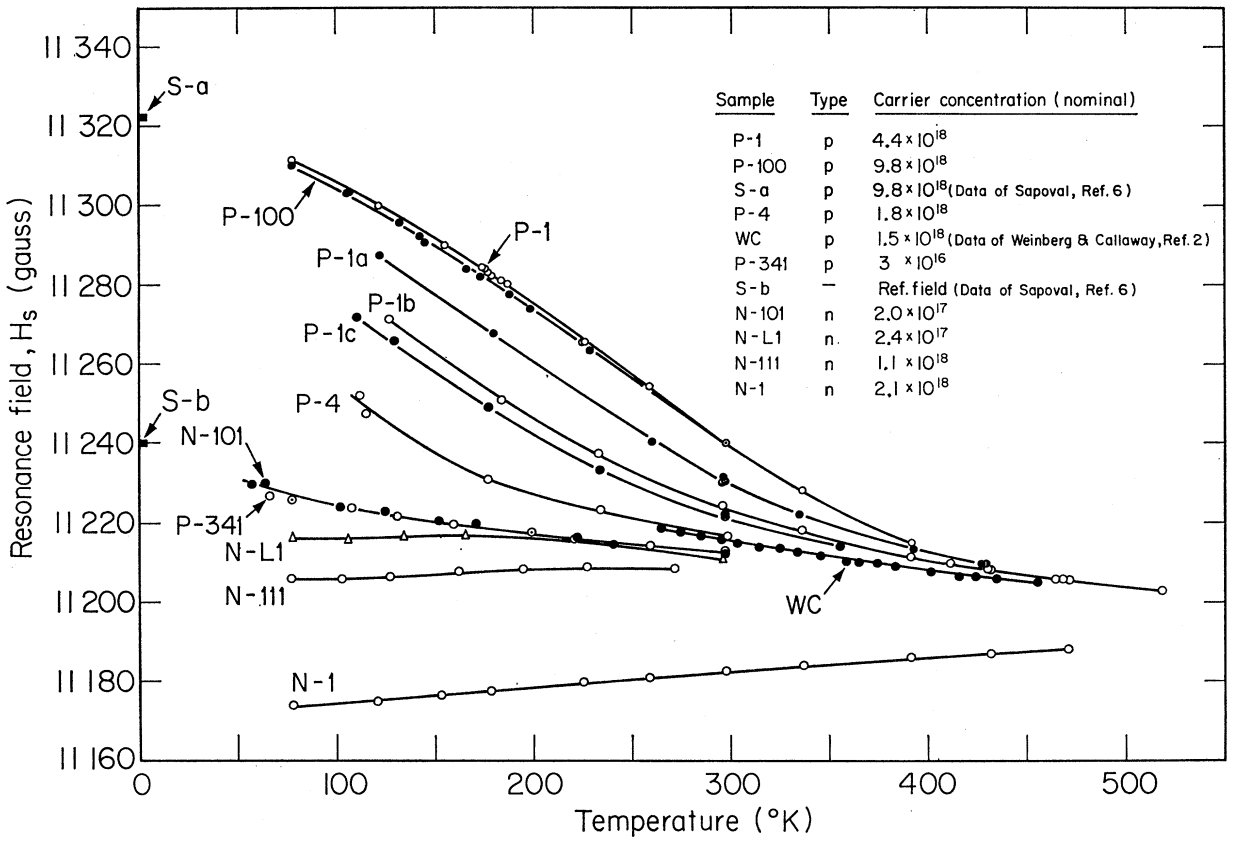

FIG. 3. Experimental data for Pb^{207} nuclear resonances in PbTe. The data have been scaled to a resonance frequency of exactly 10 MHz. The nominal carrier concentrations listed in the legend were obtained from the 100-Hz Hall coefficient measured at 77°K. The authors will supply a table of the data on request.

NMR studies in powdered specimens. Unfortunately, the production of accurately characterized PbTe samples has been and continues to be a major obstacle to the quantitative interpretation of any measurements in the lead salts. First, there have been problems of sample homogeneity which affect both bulk and powdered samples. Second, problems have been noted in sample stability, in the sense that the measured carrier concentrations have been observed to change with time. This effect has been noted elsewhere, and has been ascribed to dissolved copper-donor impurities reaching equilibrium within the sample.[27,28] Finally, for powdered specimens, there are the problems associated with damage brought about by the powdering process and the problem of one's being unable to make Hall-effect and resistivity measurements on the powdered samples. In spite of these various issues, we have been able to make Pb^{207} NMR measurements in a number of PbTe powders which, while falling short of the accurate quantitative tests we hope to make with better samples, do enable us to draw several clear and interesting inferences about the nature of the PbTe bands.

We have measured the temperature dependence of the Pb^{207} nuclear resonance in eight PbTe powders in the temperature range 55–300°K. Two of the samples have also been studied in the range 300–520°K. The measured values of the resonance field H_s are plotted against temperature in Fig. 3, scaled to a constant nuclear resonance frequency of exactly 10 MHz. Included in Fig. 3 are the data of Weinberg and Callaway[2] and two points from Sapoval's study at 1.2°K.[6] The first point is taken from his curve for p-type material with a carrier concentration of 9.8×10^{18} cm^{-3}; the second is his estimate of the reference field H_r.

The measurements on samples P-1, N-1, and P-4 were made on a conventional Varian wide-line NMR spectrometer operating in the absorption mode at a frequency of 15.3 MHz. The validity of scaling the data to 10 MHz was checked by measuring the P-1 resonance at 77°K at several lower frequencies. The ratio of resonance frequency to resonance field was independent of resonance frequency. First-derivative detection of the resonances was used; the plotted points correspond to the zero crossing of the derivative. Explicit tests

[27] R. F. Brebrick and R. S. Allgaier, J. Chem. Phys. **32**, 1826 (1960).
[28] R. F. Brebrick and E. Gubner, J. Chem. Phys. **36**, 1283 (1962).

determined that the rf level did not affect the location of the zero crossing. Measurements on the other samples (in addition to duplicate measurements on P-1, N-1, and P-4) were made at 10 MHz with a low-noise marginal oscillator spectrometer of recent design. Standard digital signal averaging techniques were used for all runs. The external field calibration was done with a self-locked NMR proton gaussmeter.[29] Temperature measurements accurate to 0.5°K for the P-1, N-1, and P-4 data were made with thermocouples embedded directly in the powdered samples; these thermocouples had been calibrated at liquid-nitrogen temperature and at the steam point. Temperature measurements on the other samples were made in a cryostat configuration which had been explicity calibrated against our own potassium-chlorate nuclear resonance thermometer.[30] Except for the characterization of the samples, the precision with which the zero crossing can be located (1 G or less) is the dominant source of experimental uncertainty.

1. Samples

For all of the samples reported on below, a Hall-effect sample was prepared from the same piece of bulk material from which the powdered NMR specimen was made. The powdering was performed as gently as possible; most samples were sieved through a 200-μ mesh making rf skin depth effects negligible. The nominal carrier concentrations listed in the legend of Fig. 3 are the inverse of qR_{77}, where R_{77} is the 77°K Hall coefficient measured at 100 Hz. Particularly for the as-grown samples (P-1, N-1, and P-4), this carrier concentration must be viewed as an estimate, because the wide NMR lines observed (see below) indicate substantial sample inhomogeneities.

The P-1 sample was taken from a p-type ingot grown by the Bridgman method. The nominal carrier concentration was 4.4×10^{18} cm^{-3}. The data between 77 and 300°K in Fig. 3 were taken before the sample was warmed above room temperature. The line was broad (10 G at room temperature, increasing to over 15 G at 77°K, measured at 15.3 MHz) and unsymmetrical, with a broad shoulder extending an additional 10 G to lower field. The broad shoulder is attributed in part to bulk sample inhomogeneities, and in part to the effects of powdering. On heating this sample to 430°K in a dry nitrogen atmosphere for the few hours needed to make NMR measurements, an irreversible shift in the room-temperature resonance was noted. The data for this changed sample, labeled P-1a in Fig. 3, were then taken between 120 and 430°K. Further heating, this time to 470°K, produced another irreversible shift in the resonance, curve P-1b. A final cycling, this time to a maximum of 520°K, produced another shift, plotted as curve P-1c. Throughout this "heat-treatment" process, the line shape underwent dramatic narrowing. The low-field shoulder became much reduced in size, and the line became narrower and more symmetrical. For the P-1c sample, the linewidth measured at a frequency of 15.3 MHz was 14 G at 110°K, decreasing to 5 G at room temperature and approaching 2.5 G at 520°K.

The P-100 sample was prepared by a vacuum-anneal technique,[31,28] starting with as-grown material similar to P-1. The Hall sample and the bulk material from which the powder was later made were annealed under vacuum for 20 min at 605°C. The resulting carrier concentration was 9.8×10^{18}, p-type, in agreement with the results of Brebrick and Gubner[28] using this technique. Note that the nominal carrier concentration compared to P-1 has doubled, while the zero crossing of the nuclear resonance has hardly moved. This is discussed below. The linewidth in this sample measured at 10 MHz was 7 G at 77°K, decreasing to 5 G at room temperature. An extrapolation of the data from this sample to 1.2°K is consistent with the data of Sapoval.

The P-4 sample was taken from an as-grown p-type ingot with a nominal carrier concentration of 1.8×10^{18} cm^{-3}. The linewidth in this sample was large, 36 G at 77°K, decreasing to 6 G at room temperature. The carrier concentration in this sample is slightly larger than in Weinberg and Callaway's sample,[2] 1.5×10^{18}. Weinberg and Callaway's data have been included in Fig. 3 for comparison purposes; their data, lying slightly below the curve for P-4, are in excellent agreement with our results.

The P-341 sample was taken from a single crystal pulled from a nonstoichiometric melt (in order to achieve low p-type carrier concentration). The particular slice from which P-341 was prepared had a Hall coefficient which changed sign between 77 and 300°K, and had a slightly nonlinear conductivity indicating that there may have been a junction in the sample. Nonetheless, the magnitude of the conductivity was very low, 4 $(\Omega\ \text{cm})^{-1}$ at 77°K, which, for typical values of the mobility (15 000 cm^2/V sec) corresponds to a carrier concentration on the order of 10^{16} cm^{-3}. The linewidth measured at 10 MHz was very narrow, 2.5 G at all temperatures. Because of the extremely low carrier concentration, we expect the resonance in this sample to be very close to the reference field H_r. An extrapolation to 1.2°K would come out about 5 G below Sapoval's estimate of H_r. We should point out, however, that Sapoval places rather broad error limits on his own estimate.[32]

The N-101 sample was annealed from a Bridgman-grown p-type ingot in a two-zone furnace. The sample was held at 700°C and a tellurium source powder was held at 174°C; total annealing time was 74 h. It was then put in a 168°C (tellurium) and 505°C (sample) two-zone furnace for 10 days. Immediately after the

[29] M. S. Adler, S.M. thesis, M.I.T., 1967 (unpublished).
[30] The techniques of potassium-chlorate nuclear resonance thermometry are discussed by D. B. Utton [Metrologia **3**, 98 (1967)].
[31] W. W. Scanlon, Phys. Rev. **126**, 509 (1962).
[32] B. Sapoval (private communication).

annealing, the sample had a carrier concentration of 1.5×10^{18}, n type. The NMR data on this sample were not taken until $1\frac{1}{4}$ yr after this annealing process. Note that the data for this sample lie essentially on top of the low concentration sample P-341. The Hall coefficient was checked, and found to correspond to a carrier concentration of 2.5×10^{17}, n type, a factor of 8 lower than the postanneal concentration. Aging of this type has been observed for samples intentionally doped with copper.[28] We attribute this partial reconversion to gradual precipitation of copper-donor impurities. The linewidth at 10 MHz in this sample was 2.5 G at all temperatures, the same as in sample P-341. Because of the location of the resonances in this sample, we suspect that the NMR powder drifted even further toward p-type material than the bulk Hall specimen.

Sample N-$L1$ also exhibited drifts over the course of a year. It was initially prepared at the Lincoln Laboratory by annealing as-grown p-type material in the presence of a lead-saturated PbTe powder for 16 h at 856°C followed by 24 h at 575°C. The carrier concentration immediately after the anneal was 4.9×10^{17}, n type. By the time the NMR sample was prepared, the carrier concentration had decreased to 2.4×10^{17}, n type. In this case, the powder was not prepared from the bulk specimen until after the year's aging had occurred, so we feel this carrier concentration to be a fairly accurate characterization of the NMR sample. The linewidth at 10 MHz was 5 G, at all temperatures.

The N-111 sample was obtained by annealing bars of as-grown p-type material at 760°C in an evacuated silica ampoule which also contained an ingot of a lead-rich alloy of lead and tellurium (70-at.% lead). The Hall coefficient showed the carrier concentration to be 1.1×10^{18} cm^{-3}, n type, which is consistent with the annealing results of Brebrick and Gubner.[28] The linewidth measured at 10 MHz was 4 G at 77°K and decreased to 3 G at room temperature.

The N-1 sample, as received, was 2×10^{18} cm^{-3}, n type; we do not know the detailed history of this sample. The linewidth measured at 15.2 MHz was broad, as in P-1, 20 G at 77°K, decreasing to 16 G at room temperature, but was less asymmetric with no shoulders or other structure. Furthermore, no aging of this sample was observed even though it was cycled through the same temperature range as P-1. Analysis by emission spectroscopy revealed iron as major impurity, on the order of 0.1%. We believe that this paramagnetic impurity has a significant effect on the location of the nuclear resonance, in that the N-1 resonance is strongly shifted in a paramagnetic direction from the resonances in the pure annealed N-111 sample. In view of the other data in n-type samples, the difference in carrier density between N-1 and N-111 is not sufficient to account for this extra paramagnetic shift.

2. *Discussion of Resonance Data*

As can be seen from the plot of H_s versus T in Fig. 3, the data indicate that the location of the Pb^{207} nuclear resonance is a strong function of carrier concentration. The one exception to a smooth variation is the inversion of the expected order of resonance field observed between samples P-100 and P-1. We attribute this anomaly to the poor quality of sample P-1, which exhibited a very broad and unsymmetrical NMR line. This kind of line shape might be expected from an inhomogeneous sample having regions with a distribution in carrier concentration. The interpretation of either the Hall coefficient or the zero crossing of the first derivative NMR signal is tenuous in a sample of this type. In neither case can one be certain that the experimental datum (Hall coefficient or zero crossing) is a correct characterization of the property of interest.

As discussed above, the resonance in the P-1 sample showed an irreversible change toward lower fields after heating. The linewidth also narrowed significantly. The aging induced by the heating can be explained in terms of the results of vacuum annealing studies of Scanlon[31] and of Brebrick and Gubner.[28] These annealing studies support the assumption that either excess lead or excess tellurium has a retrograde solubility in the PbTe matrix, and that at elevated temperatures equilibrium can be established between the excess lead (or tellurium) in solution and lead (or tellurium) in precipitation sites inside the crystal. Quenching the sample then freezes in the excess concentration corresponding to equilibrium at the annealing temperature. The excess lead or tellurium create vacancies of the opposite component in the lattice which act as donors in the case of tellurium vacancies or acceptors in the case of lead vacancies. The aging of P-1 can be understood in terms of the retrograde solubility of Te. The temperatures to which P-1, P-1a, etc., were raised during the NMR measurements corresponded to equilibrium carrier concentrations in the 10^{17} range. The time periods for which the samples were held at these slightly elevated temperatures were much too short to produce genuine equilibrium. For example, in order to obtain equilibrium at 250°C, about 100 h would be required,[31] whereas P-1c was only at this maximum temperature for a total of about 3 h. Therefore, we interpret the sequence of P-1 curves as partial approaches to a low p-type equilibrium carrier concentration. While we cannot make quantitative estimates of the actual carrier concentration at each step, we claim that the concentration decreases through the sequence P-1, P-1a, P-1b, P-1c. By the same token, the absence of any aging in the N-1 sample, which was, after all, subjected to exactly the same temperatures, can be explained in terms of the relative mobilities of Pb and Te. Equilibration times for excess Pb in n-type material are much longer,[27,28] meaning that during the few hours in which N-1 was held at elevated tempera-

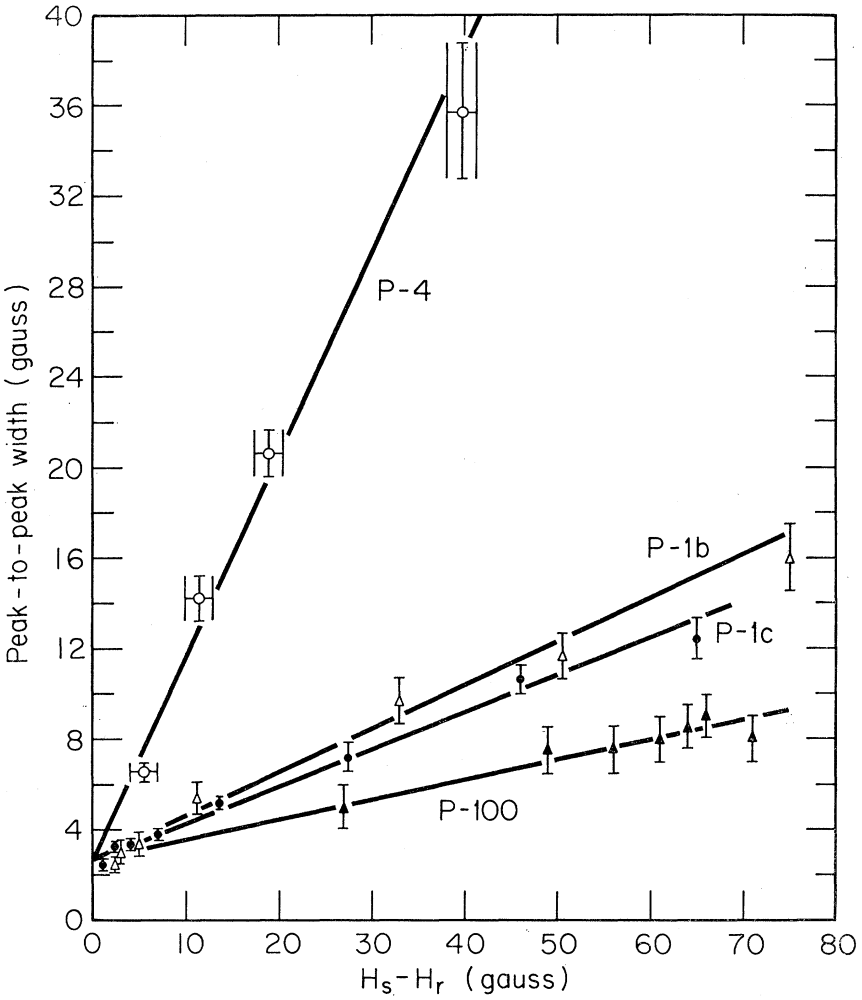

FIG. 4. Peak-to-peak linewidth of the first-derivative NMR signal as a function of Knight shift for four p-type PbTe samples. The intersection at zero Knight shift occurs at a width of 2.5 G, which is the same as the linewidth measured in sample P-341.

tures, the sample did not move very far toward equilibrium.

Since the resonance field is a strong function of carrier concentration, the linewidth should be a very good indication of the sample homogeneity. In inhomogeneous samples at low temperatures, where the dependence of H_s on n is large, one might expect to see contributions to the linewidth from the inhomogeneous broadening due to the distribution of the carrier concentration within the sample. In the simplest linear model, one would expect $\Delta H = \Delta H_0 + c(H_s - H_r)$, where ΔH is the linewidth, ΔH_0 is the linewidth in a carrier free sample, and $c(H_s - H_r)$ is a contribution proportional to the Knight shift representing the inhomogeneous broadening. The value of the slope c is a measure of the sample homogeneity. Although such a model for the linewidth is very crude, we have plotted in Fig. 4 the linewidth as a function of $(H_s - H_r)$ for samples P-1b, P-1c, P-4, and P-100. We used P-341 as a measure of H_r (see below). Note first that the linewidth data do follow roughly the model described above. It is interesting that extrapolations of the ΔH-versus-$(H_s - H_r)$ curves all fall in the neighborhood of $\Delta H_0 = 2.5$ G, the linewidth measured in the low-carrier-concentration samples P-341 and N-101. The progression of very wide linewidths in the unannealed sample P-4 to smaller linewidths in the partially annealed samples P-1b and P-1c and finally to relatively narrow linewidth in P-100, which was annealed at the highest temperature and for the longest time, is strong evidence that the annealing produces much more homogeneous samples.

3. *Interpretation of Knight Shift*

Because of the very low carrier concentration of the P-341 sample, the reference field H_r must lie within a few G of P-341 at all temperatures. The resonance in this sample, which moves from 11 227 G at 68°K down to 11 218 G at 297°K, is shifted in a paramagnetic direction by a substantial amount from resonances in other lead compounds.[33] For example, the resonance in

[33] L. H. Piette and H. E. Weaver, J. Chem. Phys. **28**, 735 (1958); J. M. Rocard, M. Bloom, and L. B. Robinson, Can. J. Phys. **37**, 522 (1959).

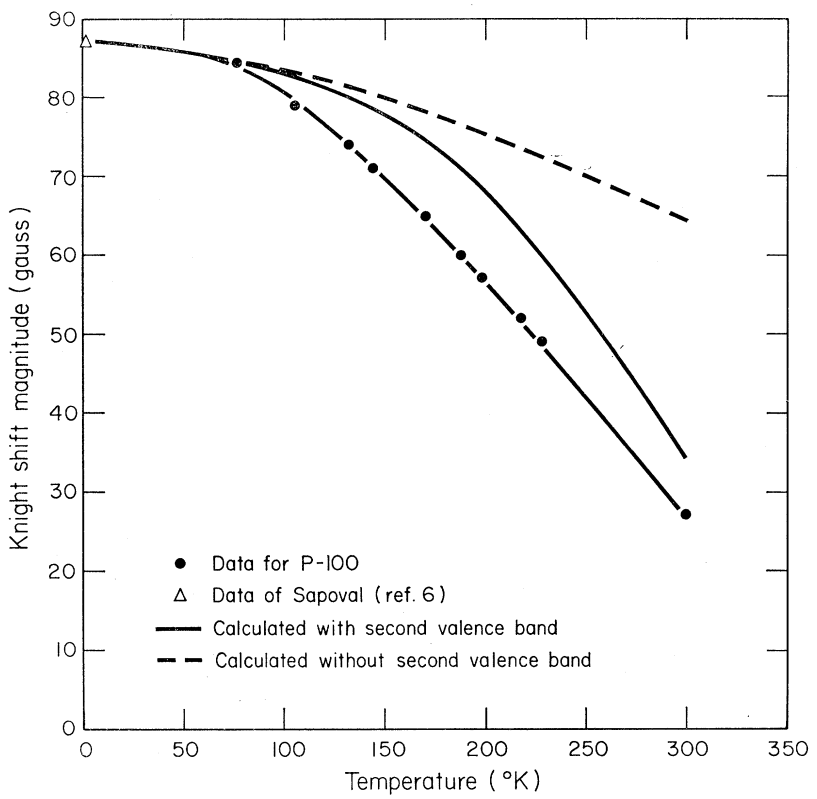

FIG. 5. Comparison of Pb^{207} NMR data in sample P-100 with the contact-interaction Knight-shift theory both with and without the second valence band. The only adjustment of the theory was a single scale factor chosen to match the experimental data at 77°K.

lead nitrate occurs at 11 267 G, a difference of 0.43%. The presence of this large paramagnetic "chemical shift" may be due to the second-order paramagnetism[34] of the filled valence and core-state bands. The fact that the reference field is temperature dependent can be attributed to the strong temperature dependences of the various energy gaps in lead telluride, because the theory of the second-order paramagnetism always involves energy gaps as denominators. The linewidth analysis of Sec. III A *2* provides interesting confirmation on the location of the reference field. If the reference field were taken more than a few G from our choice, the plots of linewidth versus Knight shift would no longer have a common intersection at zero Knight shift.

Having located the reference field, it can be seen from Fig. 3 that the Knight shift in p-type PbTe is negative ($H_r<H_s$). (Weinberg and Callaway,[2] who estimated the reference field to be at 11 242 G, assigned the opposite sign and an incorrect magnitude to the Knight shift.) The magnitude of the Knight shift, 85 G for sample P-100 at 77°K (corresponding to a shift of $K=-0.75\%$), is approximately a factor of 4 larger than our theoretical estimate. This very significant error in the estimate probably arises primarily from a failure to make a correct theoretical evaluation of the magnitude of the hyperfine coupling in lead telluride. Of course, errors in the values for the density of states and g factors will also contribute to this discrepancy. Furthermore, one might look for additional contributions to the Knight shift, such as core polarization by the d-function part of the valence-band states.[35]

Figure 3 also shows that there is a positive Knight shift in n-type material ($H_r>H_s$). The magnitude of this shift is about a factor of 4 smaller than the corresponding shift in p-type material at low temperature, although the data do not permit precise comparison. (We are ignoring the very large N-1 shift. We feel it arises at least in part from the substantial Fe concentration in that particular sample.) The fact that the shift in p-type materials is the larger shift supports the basic band model used in this paper: The valence band possesses s character around lead and produces a contact-interaction Knight shift, while the conduction band, lacking s character around the lead nucleus, can only produce smaller Knight shifts of orbital origin (see below for further discussion).

Having justified the use of the contact-interaction model as appropriate for Pb^{207} p type in lead telluride, we can conclude that the g value g_{eff} is negative for the L-point valence-band states.

The next issue involves the temperature dependence of the observed Knight shifts. The data of Fig. 3 support

[34] See, for example, C. P. Slichter, *Principles of Magnetic Resonance* (Harper and Row, Publishers, Inc., New York, 1963), pp. 69–84.

[35] Y. Yafet and V. Jaccarino, Phys. Rev. **133** A1630 (1964).

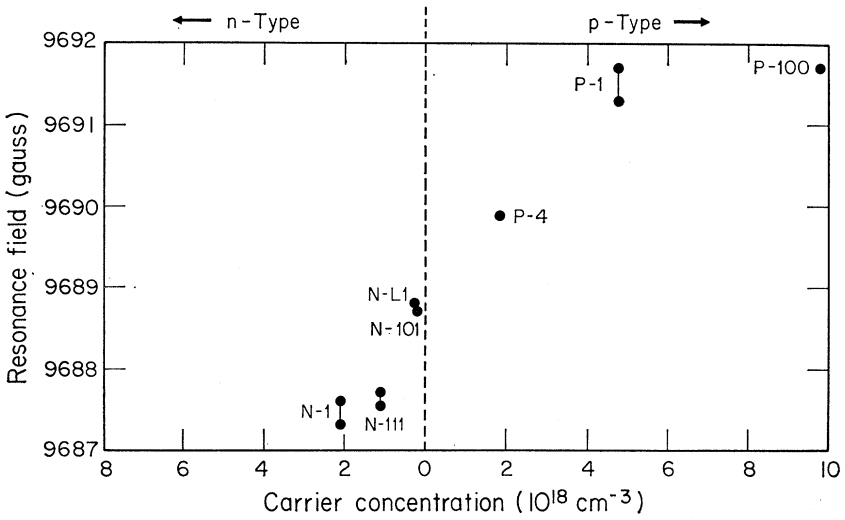

FIG. 6. Carrier-concentration dependence of the Te^{125} nuclear resonance in PbTe at 77°K. The data have been scaled to a resonance frequency of exactly 13 MHz.

the theory presented in this paper in which the motion of the Fermi level, the temperature dependence of the nonparabolic energy bands, and the presence of a second valence band are all included. At low temperatures, the holes lie in the L-point valence band, and produce a Knight shift as calculated by the contact-interaction theory developed earlier. As the material is heated, carriers shift from the L-point maximum into the second valence band. To show this effect, we have plotted in Fig. 5 a comparison of the data for sample P-100 with the second-valence-band theory of Sec. II C 5. The theory for 9.8×10^{18} carriers has been scaled by a constant factor, chosen to make the calculated Knight shift agree with the experimental Knight shift at 77°K. The dashed line in Fig. 5 represents the predicted temperature dependence for the case of the L-point valence band alone. The solid curve represents the theory including the second valence band. As can be seen, it is impossible to account for the temperature dependence of the P-100 data without including the second valence band. The large number of parameters in the model and the scarcity of well-characterized samples do not permit a precise quantitative fit of theory to experiment at this time.

Perhaps the most surprising result is the large Pb^{207} Knight shift observed in n-type material. If, as we believe, the current band model for lead telluride is correct, these shifts might arise from the localized orbital hyperfine interaction. This interaction has been discussed by Yafet[36] and subsequently by Clogston, Jaccarino, and Yafet.[37] Yafet's first discussion, which was used both by Bailey[4] and by Sapoval[6] as a basis for discounting the importance of an orbital Knight shift, explicity referred only to the long-range orbital hyperfine interaction. It explicitly excluded the short-range part of the orbital hyperfine interaction, precisely that part which, in comparison with the free-atom case, can produce substantial hyperfine couplings.[37] Estimates in these references[36,37] indicate that the short-range orbital hyperfine interaction from p or d states can be about a factor of 5 or 10 smaller than the corresponding (same shell) s-state contact interaction, a ratio not inconsistent with our results.

B. Te^{125} NMR in PbTe

We have measured the Te^{125} nuclear resonance in six of the samples at 77°K at a frequency of 13 MHz. The linewidths are all narrow, on the order of 2–3 G. The resonance field data are plotted versus nominal carrier concentration in Fig. 6, scaled to a constant NMR frequency of exactly 13 MHz. The reference field must be near 9689 G, about where the resonance occurs in the low-carrier-concentration samples N-$L1$ and N-101. We note that there are Knight shifts in both n- and p-type material, in distinct contrast to the results of Sapoval[6] who found no shift in p-type material. The Knight shift of Te^{125} in n-type material is positive. Following the band model used to interpret the Pb^{207} data, we expect a contact-interaction Knight shift in n-type material for Te^{125}. The expected magnitude of this contact-interaction shift is difficult to estimate because of the lack of hyperfine data on negatively charged ions.[38] Nonetheless, we conclude from the positive Knight shift that $g_{\text{eff}}>0$ in the conduction band. These signs for the valence- and conduction-band g factors are in agreement with the results of $\mathbf{k}\cdot\mathbf{p}$ perturbation theory.[12,13] The presence of a negative Te^{125} Knight shift in p-type material of a comparable magnitude to the positive Te^{125} shift in n-type material presents the same problem of interpretation as the Pb^{207} shift in

[36] Y. Yafet, J. Phys. Chem. Solids **21**, 99 (1961).
[37] A. M. Clogston, V. Jaccarino, and Y. Yafet, Phys. Rev. **134**, A650 (1964).
[38] W. D. Knight, in *Solid State Physics*, edited by F. Seitz and D. Turnbull (Academic Press Inc., New York, 1956), Vol. 2, pp. 93–136.

n-type material. The orbital hyperfine interaction is a possible source for this shift. The temperature dependence of the Te^{125} resonances have been measured in samples P-1, N-1, and N-111 from 77°K to room temperature. In P-1, H_s decreases by 2 G, while in N-1 and N-111, H_s increases by 1 G. The direction of the temperature dependences are consistent with the Pb^{207} data and with the theory.

C. Previous NMR work in Other Lead Salts

Except for the data of Lee, Liesegang, and Phipps,[11] no measurements have been reported in PbSe or PbS either as functions of carrier concentration or of temperature. Lee and co-workers, who studied Pb^{207} in four PbSe powders in the temperature range 183–430°K, obtained data which look very similar to our PbTe data. We differ strongly with their interpretation, in that they have failed to include correctly the motion of the Fermi level in their theory. Working within a parabolic-band approximation, they attempted an expansion of what corresponds to Eqs. (17) and (18) in the present paper, and were led by their expansion to a Knight shift which increases in magnitude with temperature instead of decreasing as we have shown. Furthermore, an extrapolation of their theory to $T=0$ led to an incorrect choice of reference field, and therefore to an incorrect determination of both the sign and the magnitude of the Knight shift. Nevertheless, their experimental data,[39] when scaled to our field and frequency, look qualitatively the same as for PbTe. For example, a p-type sample with 7.5×10^{18} carriers had a resonance field which decreased from 11 265 at 183°K to 11 230 G at 430°K. H_s decreases with increasing temperature as in our p-type samples; the magnitude of the temperature dependence is comparable. They have two n-type samples with carrier concentrations of about 10^{19} carriers both of which were heavily doped with paramagnetic impurities. The data for both these samples lie within a few G of our N-1 data, although their large scatter, on the order of 5 G, makes detailed comparison difficult. Their remaining n-type sample, had a carrier concentration of 6.3×10^{18}; the resonances in this sample lay above those in the 10^{19} samples by about 30 G at 80°K and about 15 G at 400°K. Thus the direction of the Pb^{207} Knight shift in n-type material is also the same as in PbTe. Finally, the magnitude of the over-all shift is smaller than in PbTe, a result one would expect on the basis of the smaller g factors.[12]

[39] K. Lee (private communication).

IV. SUMMARY AND CONCLUSIONS

Pb^{207} and Te^{125} Knight shifts are observed in both n- and p-type PbTe. Qualitatively similar data have been reported for Pb^{207} in PbSe. The shifts of Pb^{207} in p-type material and Te^{125} in n-type material are attributed to an s-character contact interaction with the carriers of the valence and conduction bands, respectively. The sign of the isotropic g factor g_{eff} is negative in the L-point valence band and positive in the L-point conduction band, in agreement with the results of $\mathbf{k}\cdot\mathbf{p}$ perturbation theory. The temperature dependence of the Knight shift is ascribed to the temperature dependence of the Fermi level, the temperature dependence of the energy gap and related band parameters, and to the shift in carriers from the L-point valence band to a second valence band at temperatures above about 200°K.

The source of the rather large Knight shifts of Pb^{207} in n-type material and Te^{125} in p-type material cannot be attributed to the contact interaction if the current energy-band models for the lead salts are correct. A promising alternative is the localized orbital hyperfine interaction, which can be substantial in p-like bands.

The fact that there are large Knight shifts in these materials makes NMR an interesting tool for microscopic analysis of sample inhomogeneities. The NMR linewidth can be taken as a direct measure of the homogeneity of the sample. Thus, one can expect in the future to use NMR as one of the methods of evaluating the quality of material intended for laser or other applications.

ACKNOWLEDGMENTS

The authors wish to thank Professor George W. Pratt, Professor Sohrab Rabii, and Dr. Nelson Parada for their assistance with the detailed numerical results of their APW band calculations. Professor James Walpole provided valuable advice on the handling of lead-salt samples. We are indebted to Dr. Alan Strauss of the Lincoln Laboratory, and to Dr. J. W. Moody of Battelle Memorial Institute for kindly providing some of the samples. We acknowledge valuable discussions and correspondence with Dr. Bernard Sapoval of Ecole Polytechnique. Finally, we wish to thank Dr. Michael N. Alexander for a critical reading of the manuscript, and Kenneth L. Blacker for technical assistance. Calculations were performed at the M.I.T. Computation Center.